Bed friction effects influence in shallow turbulent flows using video technology

Robles L., Jose I., Palacio P., Arturo, Rodriguez V., Alejandro

***Abstract*—** Some video techniques allows to obtain spatial and temporal flows information, in this special case, we using an video imaging method to study the effects of bed friction in shallow turbulent flows. These kinds of flows are those where the depth of flows is small compared with the horizontal length scale of the flows. Shallow shear flow of small depth is affected by friction and also by the fact that the large scale turbulence is confined to two dimensional motions. This large scale turbulence is responsible of important heat and mass exchange processes in rivers, lakes and oceans. We found in this work that only the turbulent flows in the far field are dependent of friction effects, approximately where the distance from injection of the jets is approximately $xf \cdot Cf/2l > 0.5$.

***Keywords*—J**ets, shallow flows, turbulence, video techniques.

I. Introduction

SOME important heat and mass exchange processes in rivers, lakes and oceans are associated with large-scale quasi-two-dimensional turbulent motion of shallow depth. Possibly the most important example of all shallow shear flows is the Gulf Stream in the Atlantic Ocean. With a width L of 60 km and depth h de 600 m, the horizontal to vertical length scale ratio of the Gulf Stream is also 100 to 1. The horizontal turbulent viscosity νT in the stream is estimated to be less than 100 m^2/s, [1]. The maximum speed in the stream, V, is 2 m/s. Thus the dimensionless eddy-viscosity coefficient of the Gulf stream, νT /VL ~ 0.001, is two orders of magnitude smaller than the typical value νT /VL ~ 0.1 found in free shear flows, such as in jets and mixing layers.

The quasi-two-dimensional turbulent flow consisting of large scale and the small scale turbulent motion has been the subject of a number of recent investigations. In this case, the main motion of large scale is confined to move in a predominantly horizontal direction between the free surface and the channel bed. The small movement, on the other hand, with a length scale less than the depth of the flow is three-dimensional, since it is free to move in all directions.

A lot of flows in inland and coastal are denominated shallow flows because the horizontal length scale is bigger than the vertical length scale. The water surface and the ocean bed in the shallow flow impose a restriction to move freely on the vertical way. Mainly two kind of length scales exist in shallow shear flows: The large scale turbulence produced by the horizontal shear, is confined to move in a predominantly horizontal direction between the free surface and the ocean bed. This restriction of large motion to a small depth leads to two dimensional motion. That kind of large motion is responsible of important heat and mass exchange processes in rivers, lakes and oceans. Small scale, on another hand, with a length scale less than the depth of the flow is three dimensional; since it is free to move in all directions.

This kind of studies allows obtaining information useful for turbulent modeling of the shallow shear flow.

Although attempts have been made to compare model simulations of shallow turbulent flows with experimental data [2], very few laboratory experiments of shallow turbulent flows were conducted in small depth. Recently, we were able to produce turbulent flows in a tank of small depth. The tank, as shown in figure 1, consisted of a pair of parallel walls (235 cm wide and 110 cm high) with a small space between the walls. The dye concentration in the flow was measured by a video imaging technique.

II. Experimental Set

In the experimental set we used a tank with a large lateral length scale compared with the depth. It had a ratio h/L of $4.3e^{-5}$ approximately. Quasi-two-dimensional flow produced in the tank depends on the momentum flux and buoyancy flux from the source. In the first series of the jet experiments, we take care to ensure that the water temperature of the source and the tank were equal within a measurable limit of 0.05 degree centigrade. So, the yet produced in the tank therefore is not

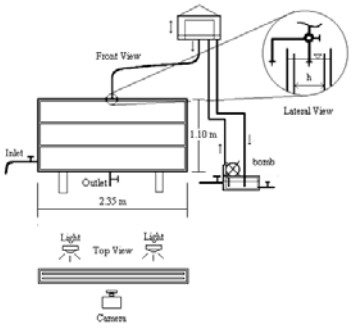

Fig. 1 Eexperimental set

affected by buoyancy force.

The momentum flux is nearly a constant in the test EXP-W1 (wide test). In this case, the depth of the flow h= $2l$ = 4.4 cm is large and the wall friction is negligible (see Figs. 15-18).

The initial development characterized by the formation of a head which is significantly greater than the jet behind. Upon impingement of the head on the bottom of the tank, the jet splits up and glides along the floor. The turbulent flow then moves up along the left and right side walls. The flows of the jets in tests EXP-N1, EXP-N2, EXP-M1, EXP-M2 and EXP-M3 are affected by friction. Friction is most important in tests EXP-N1 and EXP-N2 (narrow tests). The head of the jets in these cases stays in the mid-depth and is not able to penetrate deep enough to hit the floor (Fig. 7). The penetration is about equal to one friction length scale which is estimated in these tests to be h/cf ~ 75 cm if cf = 0.008. The depth of the water in the tank is 110 cm.

To minimize the deflection of the walls, the tank was constructed of a double wall structure. The walls, of the inner tank were kept perfectly parallel to each other by filling both the inner and outer tank with water. Wall deflection was eliminated since the net hydrostatic pressure on the inner tank walls is zero.

The outer tank walls are 125 cm high and 245 cm wide. The inner tank walls are 110 cm and 235 cm, respectively. The distance between the parallel walls in the inner tank are 4.4 cm (W), 1.29 cm (M), and 0.60 cm (N), series of tests. Table I summarizes the condition of the experiments.

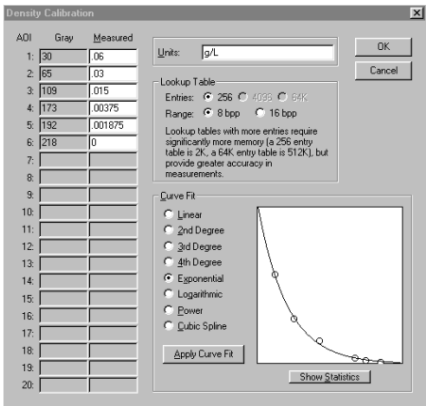

Fig. 2 calibration curve

Blue dye of known concentration was used as a tracer. The turbulent flow was illuminated by back light and recorded by a video camera (SONY 3CCD) at a rate of 30 frames per second. The video images were subsequently digitized frame by frame and analyzed using a computer.

Table I Summary of test conditions

Test	$2l$ (cm)	Q_0 (cm3/s)	C_0 (g/l)
EXP-N1	0.6	76.48	0.125
EXP-N2	0.6	62.31	0.125
EXP-M1	1.29	101.94	0.6
EXP-M2	1.29	101.94	0.06
EXP-M3	1.29	92.30	0.06
EXP-W1	4.4	68.98	0.06

The video images are stored as 24 BPP in BMP format. There are 640 x 480 pixels in a frame and each pixel has three basic colors, red, green and blue, each with values varying from 0 to 255 (see Table II). The RGB values in the BMP file are proportional to the intensities of red, green and blue light through the video camera and are related to the concentration of the dye in the turbulent flow through a calibration curve (Fig. 2 and 3).

The calibration of the video camera was conducted using diluted samples of know dye concentration. Video images were taken of the samples in a small plexiglas box of the same thickness as the inner tank and under the similar lighting condition as the experiment (Fig. 4).

Table II Color coding

red	green	blue	result
0	0	0	black
255	255	255	white
255	0	0	pure red
0	255	0	pure green
0	0	255	pure blue
X	X	X	any color

The non-linear exponential relationship is used to relate the relative dye-concentration, C/C_0 with the p-value.

The concentration of the dye in the turbulent flows of the yet is determined for each of the 640 x 480 pixels in the image file. Since the light intensity over the 110 cm x 235 cm area of the tank is not exactly uniform, the dye concentration is determined thought the change in light intensity relative to the light in the background (see Table III).

The light intensity of the background was not exactly uniform. However, by using the p-value to measure the relative light intensity, the calibration in the central region of the tank was found to be not significantly different from the calibration obtained from elsewhere in the tank.

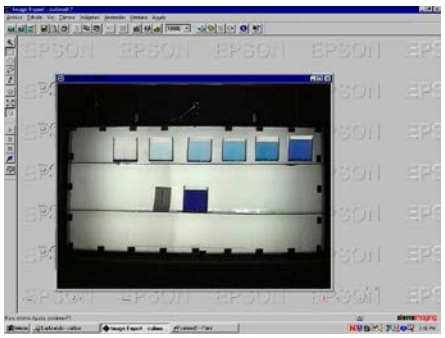

Fig. 3 Diluted samples of know dye concentration

Therefore, the dye concentration in the turbulent flow presented here was calculated based on the calibration curve obtained from a small area located in the central region of the tank.

Table III Results of test EXP-N1

No.	Dye (g)	Vol (l)	Cumulative vol.(l)	*Co* (g/l)	Color coding
1	0.125	1	1	0.1250	33
2	0.125	2	3	0.0417	107
3	0.125	2	5	0.0250	133
4	0.125	2	7	0.0179	149
5	0.125	2	9	0.0139	157
6	0.125	2	11	0.0114	164
7	0.125	2	13	0.0096	174
8	0.125	2	15	0.0083	177
9	0.125	2	17	0.0074	173
10	0.125	2	19	0.0066	176
11	0.125	2	21	0.0060	189
12	0.125	2	23	0.0054	193
13	0.125	2	25	0.0050	184
14	0.125	2	27	0.0046	204

III. Confinement Effect

Without consider the dynamical dependence of the flow on buoyancy and friction forces, turbulent motion is expected to be affected by the kinematic constraint of the walls. The energy cascade process in quasi-two-dimensional turbulent flow of shallow depth is expected to be different from the process in unconfined three-dimensional turbulent motion. Vortex stretching, the dominant mechanism in three dimensional turbulence, is absent from the process in two-dimensional motion. The kinematics of the confinement effect on the turbulent flow of shallow depth has been the subject of a number of recent investigations [3]-[5]. The results, however, were not conclusive.

The energy cascade process in quasi-two-dimensional turbulent flow of shallow depth is expected to be different from the process in unconfined three-dimensional turbulence motion. Vortex stretching, the dominant mechanism in three dimensional turbulence, is absent from the process in two dimensional motion. The kinematics of the confinement effect on turbulence flow of shallow depth has been the subject of a number of recent investigations [2]-[8].

The initial development of the turbulence jet is relatively independent of the friction effect. The inverse square concentration data follow the linear relations.

$$\frac{C_f^2}{C_m^2} = 0.103\, x_f\, \frac{c_f}{2l} \qquad (1)$$

Where $C_f{}^2$ and $C_m{}^2$ are advancing front concentration and maximum concentration respectively, c_f is the friction coefficient and $2l$ is the tank thickness.

These results are very similar those of experiment's Altai [1], with a constant value of 0.103 (1), which are the solid lines (see Figs. 4a, 4b, 4c, 4d, 4e and 4f).

IV. Turbulent Flow Friction Effect in Far Field

While the confinement effect may be negligible, the friction

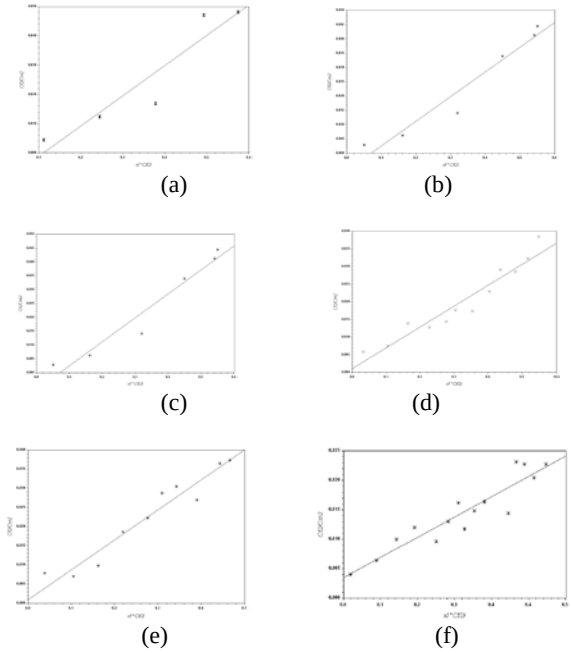

Fig. 4 a), b), c), d), e) and f) are the results of the EXP-N1, EXP-N2, EXP-M1, EXP-M2, EXP-M3 and EXP-W1 respectively in the near field

effect is not, the friction effect suppresses large scale motion. The large scale turbulent motions in the shallows flows are confined to move between the walls in a direction essentially parallel to the walls. In the far field region the mixing diminishes, so that the dye concentrations approach approximately the asymptotic values.

V. Friction Effect

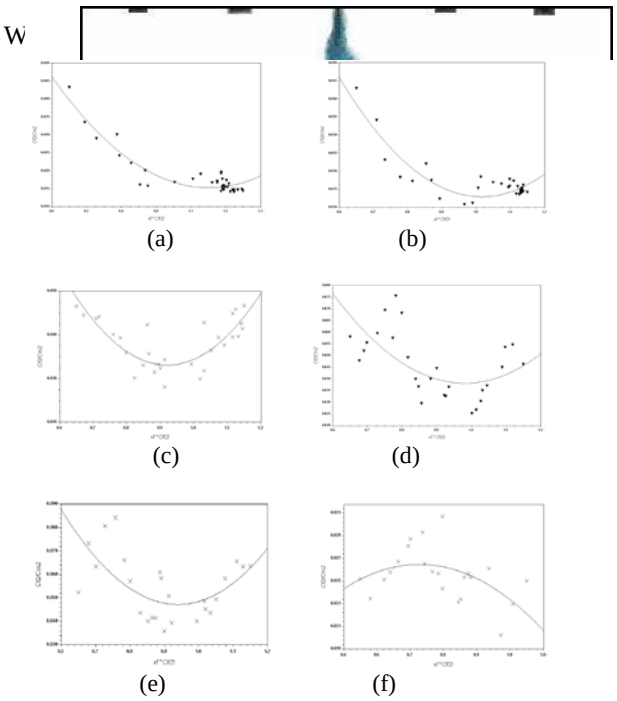

Fig. 5 a), b), c), d), e) and f) are the results of the EXP-N1, EXP-N2, EXP-M1, EXP-M2, EXP-M3 and EXP-W1 respectively in the far field.

effec
The
conc
signi
whei
two
plan
best
cond

Fig. 10 Test TN1: h=0.60 cm, t= 35 s

test EXP-W1 are free jets of the second kind; the jets in this test are confined but the friction effect is again negligible.

VI. Starting Jet

The Initial development of turbulent flow produced by the momentum source is examined in this case as a starting jet. In general, the starting jet is characterized by the formation of a 'head' which is quite large in size compared with the 'jet' of turbulent fluid that follows the head, as shown as a series of images (see Fig. 6).

The views of the starting yet are shown as a series of images (see Fig. 7-18), for the tests EXP-N1, EXP-M1 and EXP-W1 respectively. The confinement and friction effects on these starting jets depend on the depths of the flow which are $2l$ = 0.60 cm, $2l$ = 1.29 cm and $2l$ = 4.4 cm, for the three groups of tests (a) EXP-N1, EXP-N2, (b) EXP-M1, EXP-N2, EXP-M3, and (c) EXP-W1, respectively. The friction effect is likely to be negligible in the test TW with the greatest depth of $2l$ = 4.4 cm, but is expected to be significant in the test EXP-N1, EXP-N2, with the smallest depth of $2l$ = 0.60 cm.

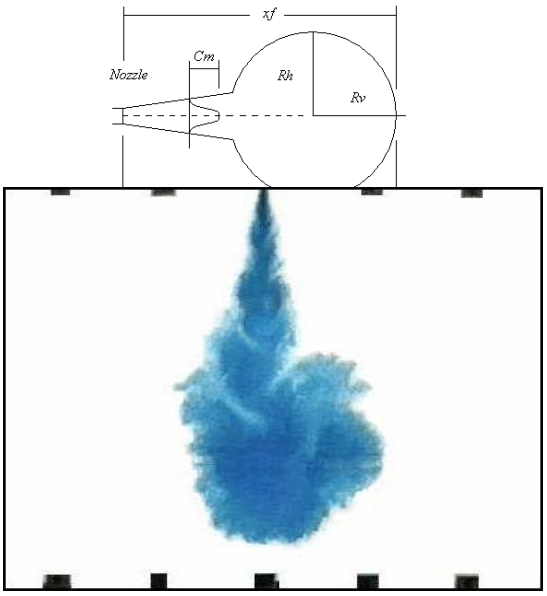

Fig. 13 Test EXP-M1: $2l$ =1.29 cm, t= 18 s

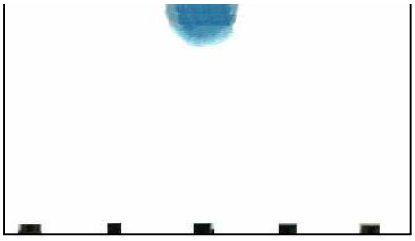

Fig. 7 Test EXP-N1: $2l$ =0.60 cm, t= 3

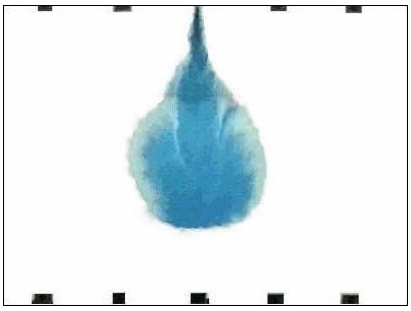

Fig. 8 Test EXP-N1: $2l$ =0.60 cm, t= 8 s

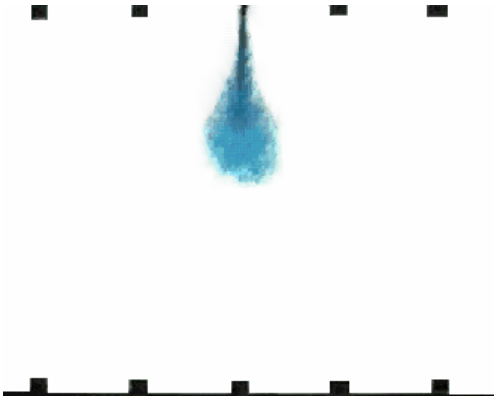

Fig. 15 Test EXP-W1: *2l*=4.4 cm, t= 3 s

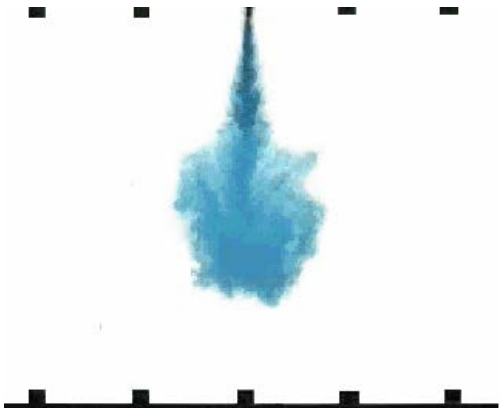

Fig. 16 Test EXP-W1: *2l* =4.4 cm, t= 8 s

Where c_f is the friction coefficient, *2l* is the inner tank thickness and C_s is the concentration scale, which is related to

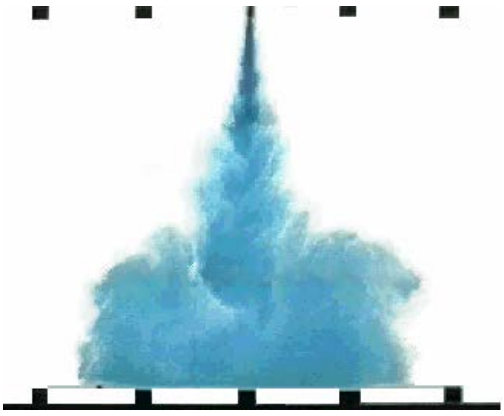

Fig. 17 Test EXP-W1: *2l* =4.4 cm, t= 18 s

Fig. 11 Test EXP-M1: *2l* =1.29 cm, t= 3 s

c_0q_0/q_s, where q_s is the discharge scale which is in terms of the momentum flux and the friction length scale as follows:

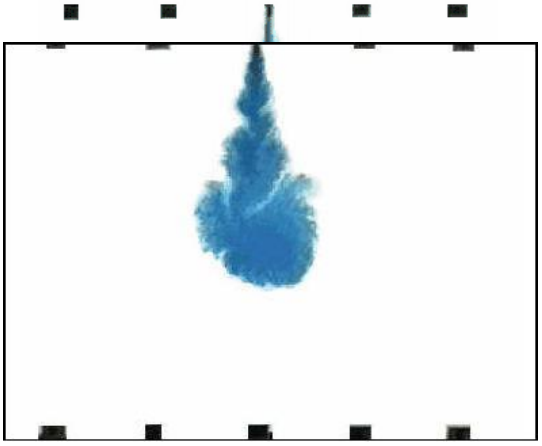

Fig. 12 Test EXP-M1: *2l* =1.19 cm, t= 8 s

$$q_s = \sqrt{\frac{2m_0 h}{\rho c_f}} \quad (2)$$

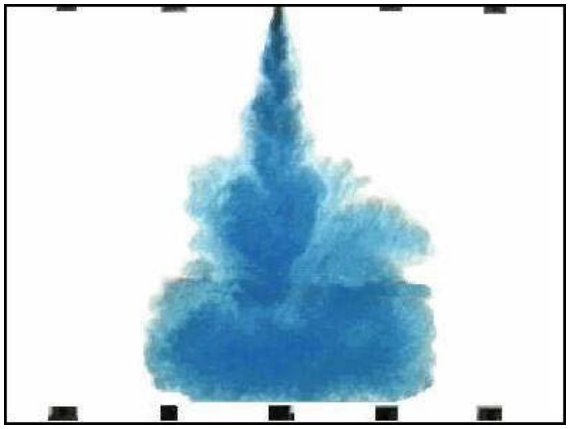

Fig. 14 Test EXP-M1: *2l* =1.29 cm, t= 35 s

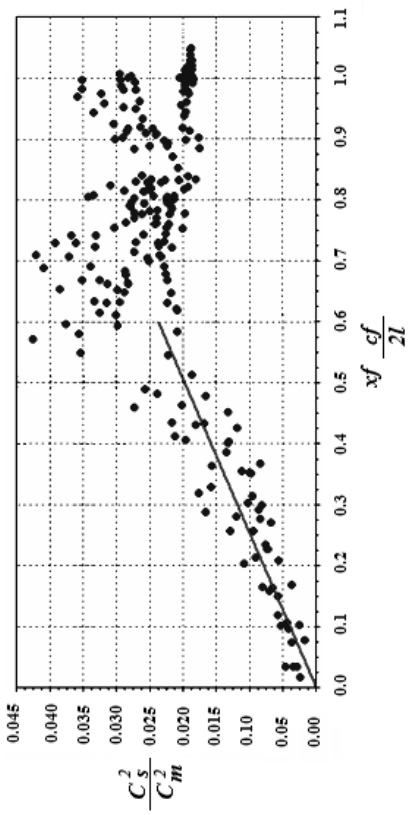

Fig. 19 Results of dye concentration maximum C_m across widest section of head. Data are inverse square of C_m normalized by concentrations scale C_s.

VIII. Far-Field Confinement Effect

Mixing diminishes in the far field region so that the dye concentration approaches the asymptotic values (3). The experimental points are scattered because they are the instantaneous values of an unsteady turbulent flow.

$$\frac{C_s^2}{C_m^2} = 0.028 \qquad (3)$$

IX. Conclusions

These results are commonly obtained by using modern experimental techniques like laser or hot wire anemometers and laser illumination planes. Image processing for the analysis of turbulent jet shallows flows was obtained by means of a PC and a video camera. The main result is that only the turbulent flow in the far field ($xf \cdot cf/2l$ > 0.5-0.6) is dependent on the friction effect of walls. In addition, we are now analyzing other turbulent quantities not still properly reported in the literature as shear stresses generated by small velocity fluctuations (double correlations) near the walls.

X. References

[1] Altai, W., Zhang, J., Chu, V. H. (1999) "Shallow Turbulent Flow Simulation Using Two-length-Scale Model (Periodical style)", *J. of Engineering Mechanics*, Vol. 125, No. 7, July, pp.780-788.

[2] Balachandar, R., Zhnag, J.B. and Chu, V.H. (1996) "Quasi-two-dimensional turbulence in the wake of a normal flat plate in shallow water, (Published Conference Proceedings style)", *Proc. Ninth Symp. On Turbulence Shear Flows*, Vol. 2, pp. 16.4.1-16.4.6.

[3] Babarutsi, S. (1991) "Modelling Quasi-two-dimensional Turbulent Shear Flow, (Thesis or Dissertation style)" Ph. D. thesis, Department of Civil Engineering, McGill University, 1991, 206 pp.

[4] Chu, V. H., Gehr, R. and Leduc, R. (1991) "Dilution of MUC wastewater treatment plant effluent in the St. Lawrence River, (Published Conference Proceedings style)", *Proc. Of the 1991 CSCE Annual Conference*, Vancouver, British Columbia. 4: 239-248.

[5] Chu, V. H. , Wu, J.-H., and Kahyat, R. E. (1983) "Stability of turbulent shear flows in shallow channels, (Published Conference Proceedings style)" *Proc. 20th IAHR Congress, Moscow*, Vol 3, pp. 128-133.

[6] Chu, V. H. , Wu, J.-H., and Kahyat, R. E. (1991) "Stability of turbulent shear flows in shallow channels, (Periodical style)", J. of Hydraulic Engineering. Vol 117, pp. 1-19.

[7] Chu, V.H. and Babarutsi, S. (1988) "Confinement and bed-friction effects in shallow turbulent mixing layers, (Periodical style)", *J. of Hydraulics Engineering, ASCE*. Vol. 114, pp. 1257-1274.

[8] Chu, V.H. and Baines, W.D. (1989) "Entrainment by a buoyant jet between confined walls, (Periodical style)", *J. of Hydraulics Engineering, ASCE*. Vol. 115, No. 4, pp. 475-492.